



# Macrophage M2 Co-expression Factors Correlate With the Immune Microenvironment and Predict Outcome of Renal Clear Cell Carcinoma

## OPEN ACCESS

Yutao Wang<sup>1†</sup>, Kexin Yan<sup>2†</sup>, Jiaying Lin<sup>1†</sup>, Jun Li<sup>1\*</sup> and Jianbin Bi<sup>1\*</sup>

**Edited by:**  
Chunjie Jiang,  
University of Pennsylvania,  
United States

<sup>1</sup> Department of Urology, The First Hospital of China Medical University, China Medical University, Shenyang, China,

<sup>2</sup> Department of Dermatology, The First Hospital of China Medical University, China Medical University, Shenyang, China

**Reviewed by:**  
Jingting Yu,  
Salk Institute for Biological Studies,  
United States  
Yi Zhang,  
Dana-Farber Cancer Institute,  
United States  
Kuixi Zhu,  
University of Arizona, United States

**Purpose:** In the tumor microenvironment, the functional differences among various tumor-associated macrophages (TAM) are not completely clear. Tumor-associated macrophages are thought to promote the progression of cancer. This article focuses on exploring M2 macrophage-related factors and behaviors of renal clear cell carcinoma.

**Method:** We obtained renal clear cell carcinoma data from TCGA-KIRC-FPKM, GSE8050, GSE12606, GSE14762, and GSE3689. We used the “Cibersort” algorithm to calculate type M2 macrophage proportions among 22 types of immune cells. M2 macrophage-related co-expression module genes were selected using weighted gene co-expression network analysis (WGCNA). A renal clear cell carcinoma prognosis risk score was built based on M2 macrophage-related factors. The ROC curve and Kaplan–Meier analysis were performed to evacuate the risk score in various subgroups. The Pearson test was used to calculate correlations among M2 macrophage-related genes, clinical phenotype, immune phenotype, and tumor mutation burden (TMB). We measured differences in co-expression of genes at the protein level in clear renal cell carcinoma tissues.

**\*Correspondence:**

Jianbin Bi  
bjjianbin@hotmail.com  
Jun Li  
cmu\_ljliun@163.com

**Results:** There were six M2 macrophage co-expressed genes (F13A1, FUCA1, SDCBP, VSIG4, HLA-E, TAP2) related to infiltration of M2 macrophages; these were enriched in neutrophil activation and involved in immune responses, antigen processing, and presentation of exogenous peptide antigen via MHC class I. M2-related factor frequencies were robust biomarkers for predicting the renal clear cell carcinoma patient clinical phenotype and immune microenvironment. The Cox regression model, built based on M2 macrophage-related factors, showed a close prognostic correlation (AUC = 0.78). The M2 macrophage-related prognosis model also performed well in various subgroups. Using western blotting, we found that VSIG4 protein expression levels were higher in clear renal cell carcinoma tissues than in normal tissues.

<sup>†</sup>These authors have contributed equally to this work

**Specialty section:**

This article was submitted to  
Computational Genomics,  
a section of the journal  
Frontiers in Genetics

**Received:** 09 October 2020

**Accepted:** 07 January 2021

**Published:** 22 February 2021

**Citation:**

Wang Y, Yan K, Lin J, Li J and Bi J  
(2021) Macrophage M2  
Co-expression Factors Correlate With  
the Immune Microenvironment and  
Predict Outcome of Renal Clear Cell  
Carcinoma. *Front. Genet.* 12:615655.  
doi: 10.3389/fgene.2021.615655

**Conclusion:** These co-expressed genes were most related to the M2 macrophage phenotype. They correlated with the immune microenvironment and predicted outcomes of renal clear cell carcinoma. These co-expressed genes and the biological processes associated with them might provide the basis for new strategies to intervene via chemotaxis of M2 macrophages.

**Keywords:** M2 macrophage, weighted gene co-expression network analysis, tumor-associated macrophage, immune phenotype, risk model

## INTRODUCTION

Renal clear cell carcinoma (RCC) accounts for 80–90% of all renal cell carcinomas; clear cell carcinoma is not sensitive to chemotherapy and radiotherapy (Hsieh et al., 2017). For this reason, radical surgery has become the main treatment method. In clinical practice, although radical nephrectomy can benefit mostly patients, 30% of patients experience distant metastases after surgery (Motzer et al., 2013). Although we have adopted various treatment strategies for these patients with poor status, the long-term outcomes are not ideal (Linehan and Ricketts, 2019). With the development of immunotherapy in recent years, there have been studies showing that immunotherapy can benefit patients with renal clear cell cancer (Chowdhury and Drake, 2020; Díaz-Montero et al., 2020; Wang C. et al., 2020).

Renal clear cell carcinoma is characterized by many new tumor antigen peptides and high mutation burden; it is relatively sensitive to immunotherapies such as targeting PD1 and PD-L1 (Wang C. et al., 2020). Immune regulation plays a crucial role in the renal clear cell carcinoma microenvironment. This process includes immune checkpoints [mainly programmed cell death 1 (PD-1) and programmed cell death 1 ligand 1 (PD-L1)], as well as regulatory T cells, the original source of suppressor cell tumor-associated macrophages, and type 2 innate and adaptive lymphocytes (Xu W. et al., 2020). Macrophages in the primary or secondary tumor tissues are called tumor-associated macrophages (TAMs); these are the largest number of macrophages in the tumor stroma (Herberman et al., 1979). In recent years, clinical and experimental evidence has shown that macrophages promote the progression and metastasis of solid tumors, and this is somewhat different from our previous understanding (Pollard, 2004; Karnevi et al., 2014). Tumor-associated macrophages are divided into two types, M1 and M2 (Herberman et al., 1979; DeNardo and Ruffell, 2019). The biological effects of the two types are exact opposites. As tumors progress, increasing numbers of M2 macrophages appear, resulting in a weaker antigen presentation effect. For this reason, targeting macrophages has become a new therapeutic strategy (DeNardo and Ruffell, 2019). M1 type macrophages, namely, classically activated macrophages, highly express IL-12 and IL-23 that enhance antitumor effects (Lawrence and Natoli, 2011). By

contrast, M2 type macrophages, namely, alternatively activated macrophages, promote tumor formation and development (Cervantes-Villagrana et al., 2020). The mechanism of this polarization of macrophages is not clear. This article focuses on exploring the M2 macrophage-related genes in renal clear cell cancer, and constructing co-expression networks of M2 macrophages using the WGCNA method. The results of this paper revealed the underlying interaction mechanisms of M2 macrophage co-expressing factors and explained the role of M2 macrophages in the immune microenvironment from the perspective of bioinformatics.

## METHODS

### Macrophage M2, Tumor Purity, and Tumor Mutation Burden Evaluation

We downloaded The Cancer Genome Atlas TCGA—KIRC FPKM data (<http://cancergenome.nih.gov/>) containing 539 renal clear cell cancer tissue samples and 72 normal tissues. GSE8050 (Weinzierl et al., 2008), GSE12606 (Stickel et al., 2009), GSE14762 (Wang et al., 2009), and GSE36895 (Peña-Llopis et al., 2012) were also downloaded from the GEO (<http://www.ncbi.nlm.nih.gov/geo/>) database. The Robust Multi-Array Average (RMA) algorithm of the “sva” (Leek et al., 2012) package was used to remove batch effects among the four GEO cohorts. The TCGA cohort was used to select M2-related genes. Four GEO cohorts were combined using “sva” packages and to verify the results. The Cell type Identification By Estimating Relative Subsets Of RNA Transcripts (CIBERSORT) is a deconvolution algorithm based on a gene expression profile that characterizes the cell composition of complex tissues, quantifies immune cells, and accurately estimates the immune components of tumor samples. It expands the potential of the genomic database, showing the pattern of Renal Clear Cell Carcinoma with comprehensive immune cells. We calculated macrophage M2 cell proportions based on the LM22 matrix using the CIBERSORT (Chen et al., 2018) algorithm. Cibersort was used as an obvious method to evaluate the significance of infiltration of immune cells in the samples. The assessment results of some samples were not statistically significant, and we used  $P < 0.05$  to screen the samples. The Estimation of Stromal and Immune cells in Malignant Tumor tissues using Expression data (ESTIMATE) is a method that infers the fraction of stromal and immune cells using gene expression signatures (Yoshihara et al., 2013). Using the ESTIMATE package, we calculated tumor purity in each renal

**Abbreviations:** TCGA, The Cancer Genome Atlas; GEO, Gene Expression Omnibus; BLCA, Bladder urothelial carcinoma; ROC, Receiver operating characteristic; AUC, Area under the curve; HR, Hazard ratio; TME, Tumor microenvironment.

clear cell cancer sample. TMB (tumor mutation burden) per megabyte is calculated by dividing the total number of mutations by the size of the target coding region (Li et al., 2020; Yang et al., 2020).

## Macrophage M2 Co-expression Network Conduction

Weighted gene co-expression network analysis (WGCNA) is a system biology approach that converts co-expression correlations

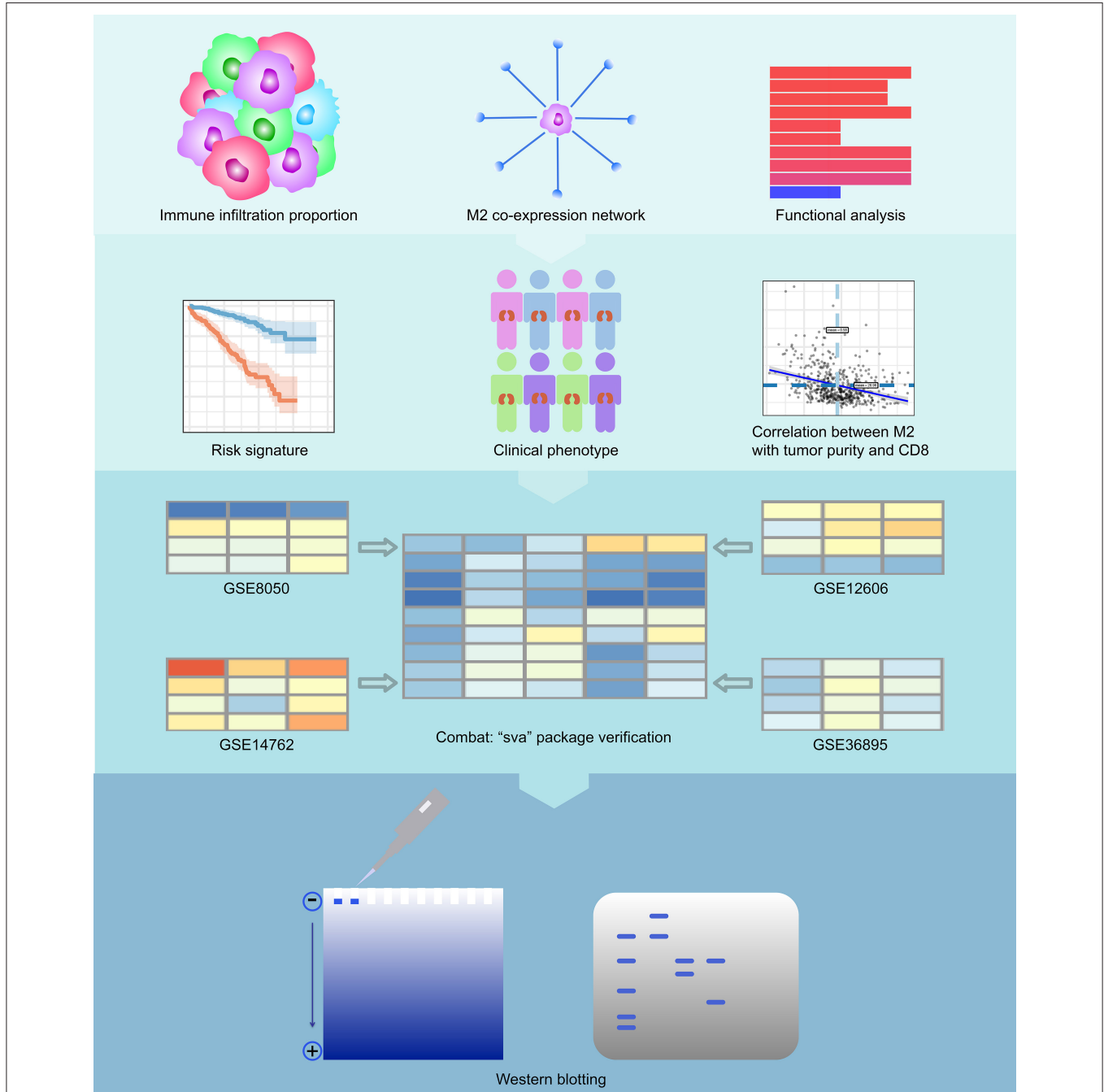


**FIGURE 1** | Flowchart of the experimental design. We first calculated immune infiltration to determine the content of M2 macrophages in the immune microenvironment of RCC. Then, we constructed a co-expression network related to M2 macrophages of RCC and analyzed the enriched pathways in this network. We then calculated the survival analysis of these co-expressed genes. We constructed a COX regression prognostic model associated with the co-expression genes of M2 macrophages in RCC and performed a subgroup analysis of this model. We analyzed the relationship between key genes in the model and tumor purity and CD8<sup>+</sup> T cells. Finally, we also verified the feasibility of the model with 4 GEO datasets and conducted western blotting experiments on VSIG4.

into connection weights or topology overlap values (Langfelder and Horvath, 2008). We used this method to determine proportions of co-expressed genes in the M2 macrophage. The expression patterns are similar for genes with the same biological process and biological function (Jiang et al., 2017). We built a scale-free topology network, set the soft threshold at 5,  $R$  square = 0.89, and set the number of genes in the minimum module at 30. The M2 macrophage cell proportion was considered for phenotype files in WGCNA. In this manner, a cluster of M2 macrophage cell proportion-related genes with similar function were identified in the same module. The factors with M2 macrophage correlation >0.4 in the most relevant modules were determined.

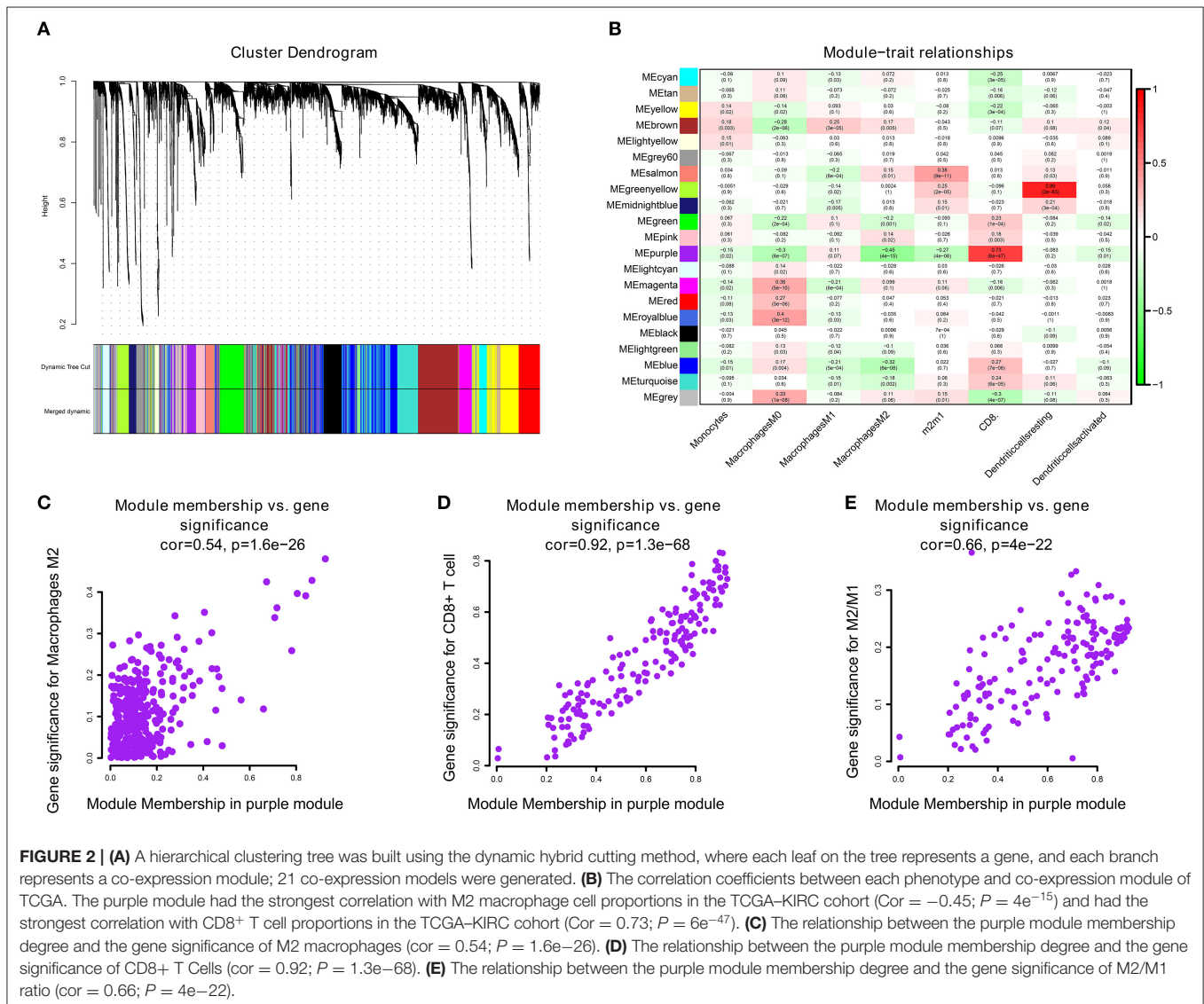
### M2 Macrophage-Related Module Analysis

The genes were selected using  $|\text{correlation coefficient}| > 0.4$ . The Database for Annotation, Visualization and Integrated Discovery (DAVID, v6.8) is an open-source database that performs

function enrichment (Huang et al., 2007). We used the Kyoto Encyclopedia of Genes and Genomes (KEGG) (<https://www.genome.jp/kegg/>) (Kanehisa et al., 2017) and Gene Ontology (GO) (<http://geneontology.org/>) analysis (Ashburner et al., 2000) to identify the biological function in each co-expression module. In this way, we identified the biological processes associated with M2-type macrophage proportion.

### M2 Macrophage-Related Genes Analysis

To verify the correlation between these factors and the clinical phenotype, we measured the overall survival from clear cell carcinoma as the prognostic indicator. Survival analysis was performed to evaluate the prognostic value of these co-expressed factors in M2 macrophages. Subsequently, a Cox regression hazard model was built based on the M2 macrophage-related genes. Next, we generated a model validation of clinical subgroups, which was based on age, gender, tumor metastasis, tumor stage, tumor purity, and degree of tumor mutation



burden. In different subgroups, we evaluated the predictive abilities of M2 macrophage-related prognostic models. Finally, we calculated tumor purity in TCGA samples and explored the correlations between macrophage-related factors and tumor purity.

## HPA

To verify the protein expression levels of candidate genes in melanoma and normal tissues, the human protein atlas (HPA, <https://www.proteinatlas.org/>) database was used to demonstrate differences in co-expressed genes at the protein level (Uhlén et al., 2015).

## Western Blotting

Thirty clear renal cell carcinoma tissue samples were obtained from patients who underwent Nephrectomy at the First Affiliated Hospital of China Medical University. This study was authorized by the Ethics Committee of the First Affiliated Hospital of China Medical University. All patients signed informed consent. Protein extraction and western blotting were conducted as described previously (Prupp, 2018). An antibody against VSIG4 was purchased from Sigma-Aldrich.

## Statistical Methods

Pearson correlation coefficients measure the strength of the linear relationship between two variables. The correlation coefficients

are  $-1$  to  $+1$ , respectively, indicating negative correlation and positive correlation, respectively, while  $0$  indicates no correlation (Wang Y. et al., 2020). The key factors in the model score, tumor purity, tumor mutation burden, M2 macrophages, and CD8<sup>+</sup> T lymphocytes were assessed using this test.

## RESULTS

### M2 Macrophages, Tumor Purity, and Tumor Mutation Burden

The results of our methodology are explained in **Figure 1**.

We summed up the following clinical data composed by M2 macrophages, tumor mutation burden, and clinical following survival data. M2, and M1, and M2/M1 macrophages were inputted as phenotype files to WGCNA. The detailed information is displayed in **Supplementary Table 1**.

### M2 Macrophages Co-expression Network Conduction

We performed WGCNA analysis with TCGA-KIRC. A hierarchical clustering tree was built using the dynamic hybrid cutting method, where each leaf on the tree represents a gene, and each branch represents a co-expression module; 21 co-expression models were generated (**Figure 2A**). The correlation coefficients

**TABLE 1** | The Module and gene significance for M2 macrophage-related genes in the purple module.

ID	moduleColor	GS.MacrophagesM2	p.GS.M2	GS.CD8.T	p.GS.CD8.
CD27	purple	-0.497	1.32E-18	0.774	2.91E-56
PSMB9	purple	-0.493	2.94E-18	0.715	1.65E-44
CTSW	purple	-0.488	7.07E-18	0.787	2.57E-59
CD3E	purple	-0.483	1.57E-17	0.734	6.70E-48
CST7	purple	-0.482	1.77E-17	0.799	2.39E-62
CD3D	purple	-0.480	2.90E-17	0.755	5.32E-52
SIT1	purple	-0.479	3.05E-17	0.753	1.02E-51
HLA-F	purple	-0.476	5.88E-17	0.689	3.94E-40
IL2RG	purple	-0.475	6.28E-17	0.649	2.22E-34
GZMA	purple	-0.468	2.22E-16	0.7789	2.89E-57
NKG7	purple	-0.468	2.22E-16	0.762	1.28E-53
CD8B	purple	-0.467	2.28E-16	0.832	6.65E-72
PRF1	purple	-0.466	2.80E-16	0.744	9.06E-50
CD8A	purple	-0.466	2.93E-16	0.830	3.40E-71
LCK	purple	-0.465	4.62E-16	0.694	2.54E-42
APOBEC3G	purple	-0.461	6.88E-16	0.715	2.18E-44
HLA-B	purple	-0.459	9.61E-16	0.682	4.66E-39
CXCR3	purple	-0.458	1.03E-15	0.684	2.29E-39
IRF1	purple	-0.457	1.30E-15	0.671	2.24E-37
CD2	purple	-0.449	4.11E-15	0.729	6.85E-47
DUSP2	purple	-0.449	4.43E-15	0.763	1.13E-53
CCL5	purple	-0.447	5.76E-15	0.588	4.94E-27
HLA-E	purple	-0.423	1.08E-14	0.688	1.58E-35
PSME2	purple	-0.409	1.98E-14	0.525	1.11E-43

GS, Gene significance.

between each phenotype and co-expression module of TCGA are shown in **Figure 2B**. The results showed that the purple module had the strongest negatively correlation with M2 macrophage cell proportion in the TCGA-KIRC cohort ( $Cor = -0.45$ ;  $P = 4e^{-15}$ ) and had the strongest correlation with CD8<sup>+</sup> T cell proportion in the TCGA-KIRC cohort ( $Cor = 0.73$ ;  $P = 6e^{-47}$ )

(**Figure 2B**). Based on these findings, we have supplemented the scatter plots of the correlation between the factors in the purple module (**Figures 2C–E**). The horizontal axis is the correlation between the gene and the module, which is used to measure the relationship between the gene and the co-expression module, and the vertical axis is the correlation between the gene and the

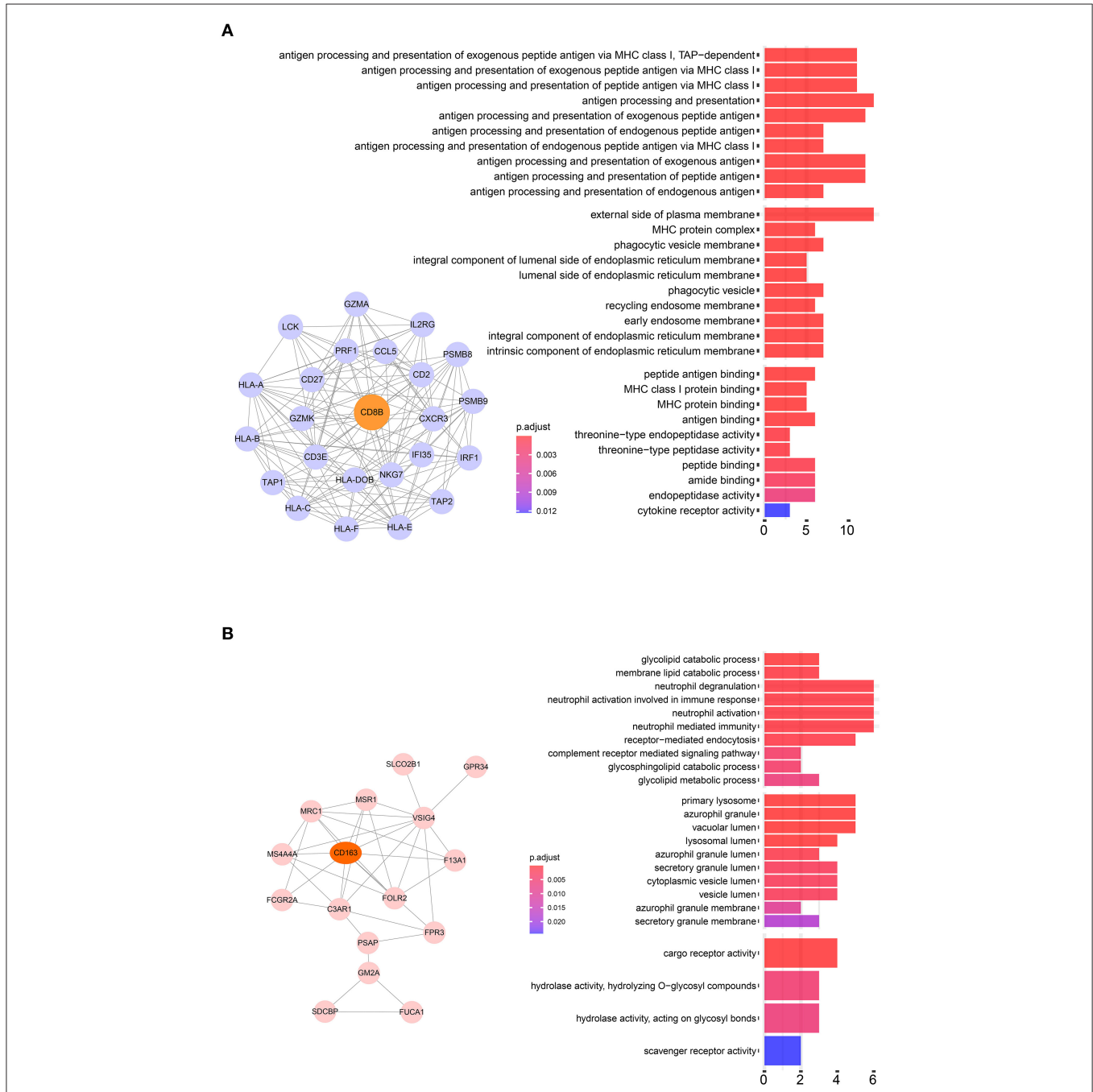


**FIGURE 3 | (A)** Pathway analysis of 24 negatively correlated co-expressed genes in M2 macrophages in the purple module. These genes were most significantly enriched in the antigen processing and presentation of exogenous peptide antigen via MHC class I, which suggested a declining effect on tumor antigen peptide process. **(B)** Pathway analysis of 16 negatively correlated co-expressed genes in M2 macrophages in the brown module. These genes were most significantly enriched in neutrophil activation involved in immune responses.

macrophage. By drawing the scatter diagram above, we screened out genes that are related to both M2 macrophages and the co-expression module.

### M2 Related Genes Function Analysis

Twenty-four M2 macrophage negatively co-expressing genes were identified with coefficient <-0.4 in the TCGA-KIRC purple module. The gene significance for M2 macrophage-related genes in the purple module is shown in **Table 1**. Top 20 M2 macrophage cell proportion positively co-expressing genes were identified in the TCGA-KIRC pink module. The 24 M2 macrophage negatively co-expressing genes were most significantly enriched in the antigen processing and presentation of exogenous peptide antigen via MHC class I, which suggested a declining effect on the tumor antigen peptide process (**Figure 3A**). The 20 M2 macrophage negatively co-expressing genes were most significantly enriched in neutrophil activation involved in immune responses (**Figure 3B**).

### M2 Related Genes Prognosis Analysis

To analyze their influence on overall survival, we performed survival analysis. F13A1, FCGR2A, HLA.DOB, ILR2GHLA, DUSP2, PSME2, CD27, IFI35, LIMD2, NFKB2, IL2RB, CCL5, VSIG4, APOBEC3G, GZMA, and PSMB10 were prognosis risk factors for clear renal cell carcinoma. HLA-E, MRC1, GPR34, KCTD12, LIPA, PSAP, MFSD1, EHD1, FUCA1, and CPVL

**TABLE 2 |** The Module and gene significance for M2 macrophage-related genes in the pink module.

ID	moduleColor	GS.MacrophagesM2	p.GS.M2
GPR34	pink	0.467	2.31E-16
MS4A4A	pink	0.452	2.93E-15
MFSD1	pink	0.446	6.88E-15
FUCA1	pink	0.435	3.55E-14
CD163	pink	0.428	1.07E-13
FOLR2	pink	0.427	1.13E-13
LIPA	pink	0.424	1.78E-13
SLCO2B1	pink	0.418	4.43E-13
PSAP	pink	0.415	6.44E-13
SDCBP	pink	0.404	3.17E-12
C3AR1	pink	0.395	9.95E-12
F13A1	pink	0.391	1.60E-11
KCTD12	pink	0.386	3.14E-11
MSR1	pink	0.384	4.12E-11
CPVL	pink	0.365	4.15E-10
FCGR2A	pink	0.362	5.48E-10
FPR3	pink	0.358	9.40E-10
GM2A	pink	0.353	1.68E-09
VSIG4	pink	0.347	3.12E-09
MRC1	pink	0.337	9.28E-09

GS, Gene significance.

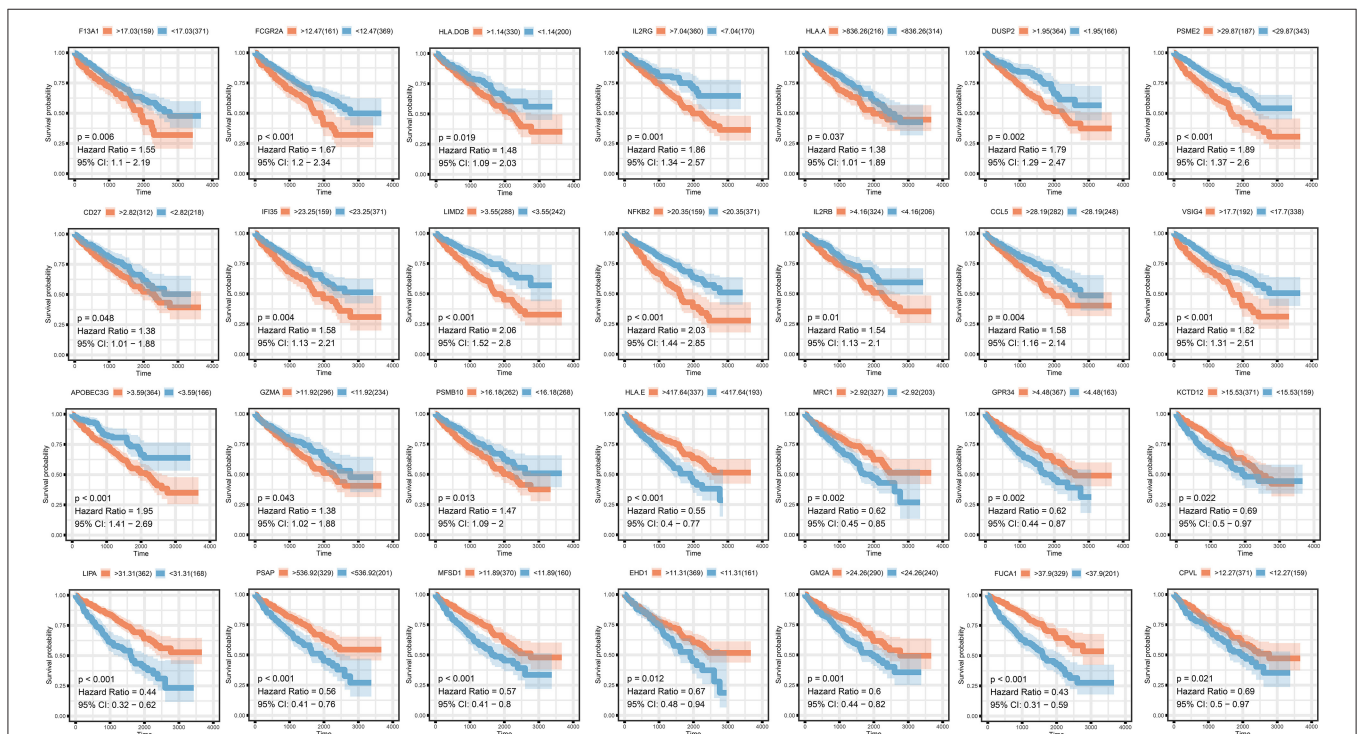


**FIGURE 4 |** Survival analysis of selected co-expressed genes in purple and pink modules.

were prognosis-protective factors for clear renal cell carcinoma (Figure 4).

### M2 Macrophage-Related Prognosis Signature

We then generated a multi-Cox regression risk score model based on M2 macrophage-related genes (Tables 1, 2). Risk

score = 0.025 \* F13A1 - 0.008 \* FUCA1 + 0.034 \* FCGR2A - 0.016 \* KCTD12 - 0.08 \* MFSD1 - 0.003 \* HLA-E + 0.012 \* SDCBP - 0.071 \* MRC1 - 0.086 \* LCK + 0.02 \* PSME2 + 0.016 \* VSIG4 + 0.215 \* TAP2. Detailed information of the prognosis model is displayed in Supplementary Table 2. The patients in high-risk groups for renal clear cell cancer (TCGA:  $P < 0.001$ ; HR = 5.31) (Figure 5) showed survival risk vs. low

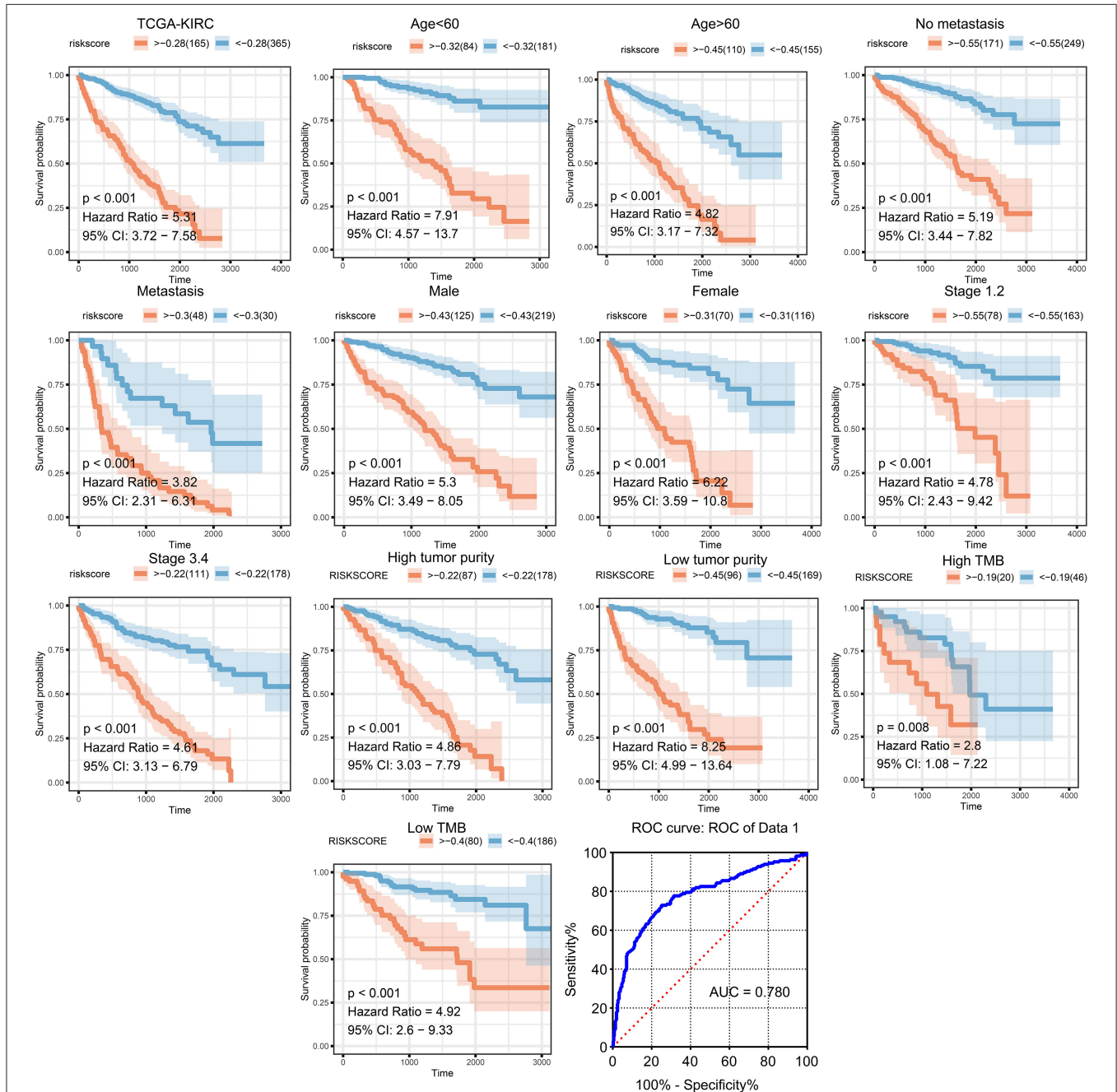


**FIGURE 5 |** Validation of the prognostic model in clinical subgroups. The patients in high-risk groups for renal clear cell cancer (TCGA:  $P < 0.001$ ; HR = 5.31) showed survival risk against low expression groups, with the area under curve (AUC) = 0.780. The risk score was evaluated in clinical subgroups, including age, gender, stage, metastasis, tumor purity, and tumor mutation burden. P-values of all subgroups validations were  $< 0.05$ , indicating that this model has good predictive ability.

expression groups, with the area under the curve (AUC) = 0.780 (Figure 5). The risk score was evaluated in various subgroups, including age, gender, stage, metastasis, tumor purity, and tumor mutation burden. The results were significant in these subgroups (Figure 5).

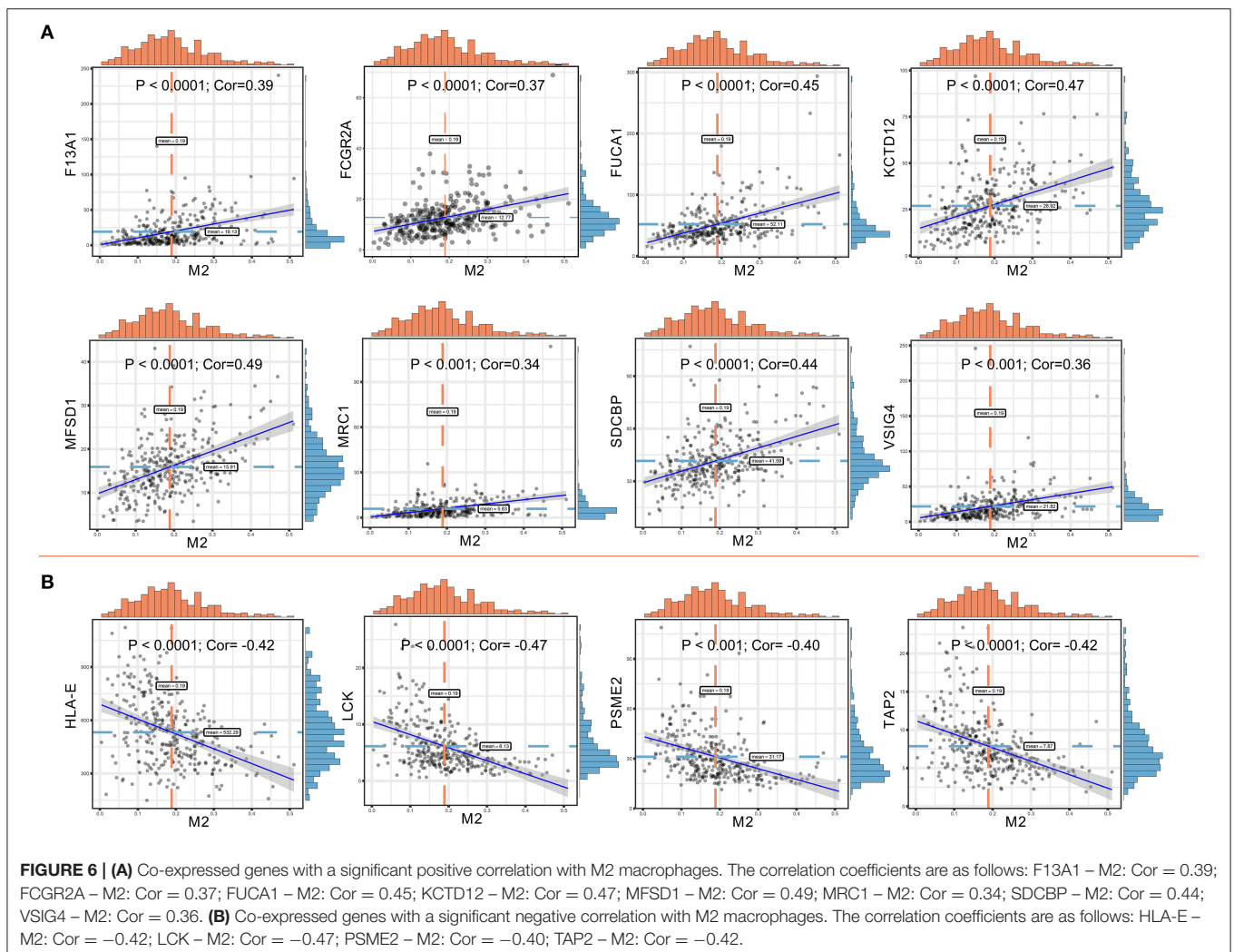
## Immune Environment Correlation

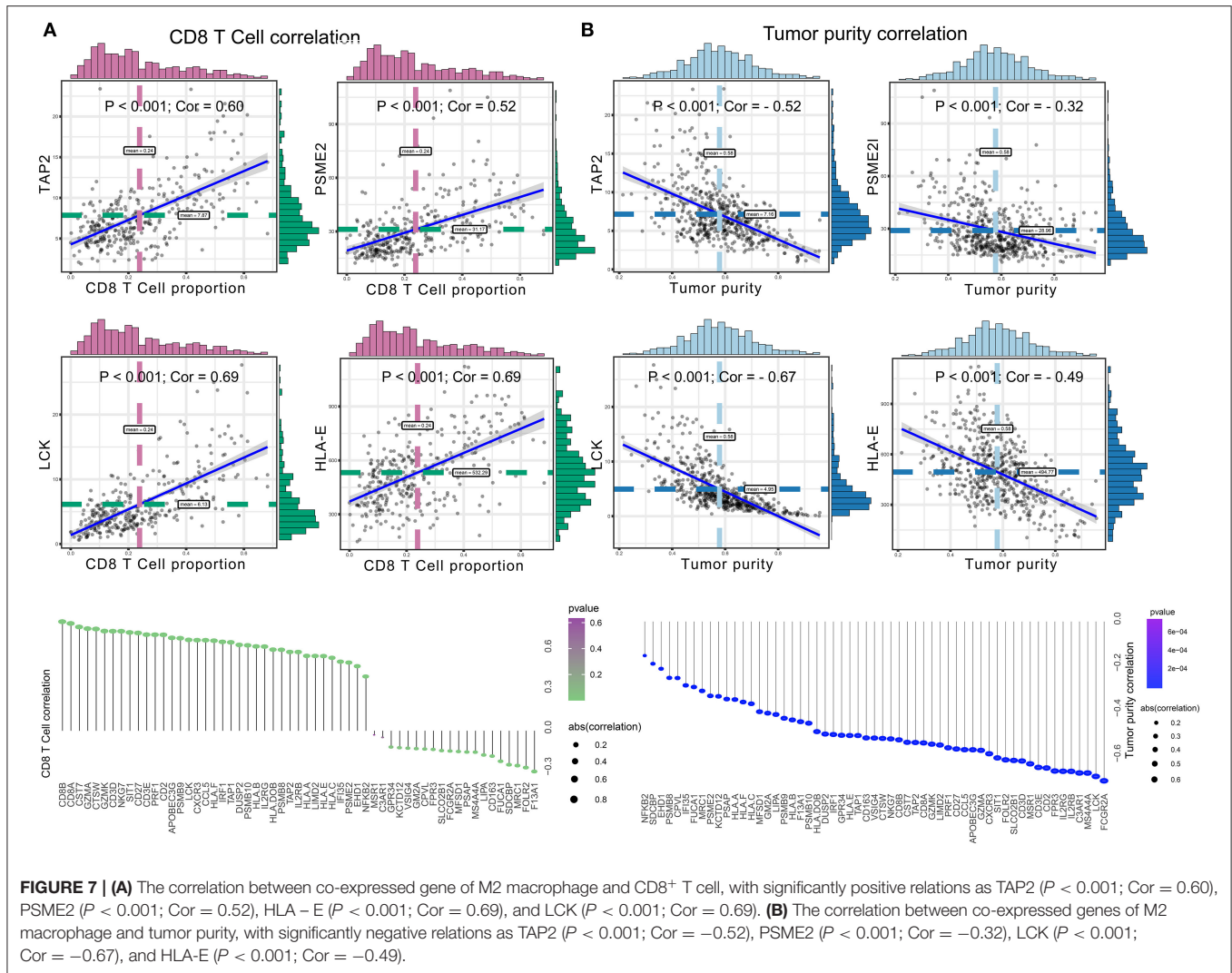
Significant associations between M2 frequency and the genes involved in the risk signature are indicated in Figure 6, and the highest correlation of MFSD1 was 0.49 (Figure 6A); the correlation of LCK was the lowest at  $-0.47$  (Figure 6B). TAP2, PSME2, HLA-E, and LCK were negatively related to M2 macrophage proportions. We then analyzed the correlations with CD8<sup>+</sup> T cell and tumor mutation burden of these four genes. TAP2 ( $P < 0.001$ ; Cor = 0.60), PSME2 ( $P < 0.001$ ; Cor = 0.52), HLA - E ( $P < 0.001$ ; Cor = 0.69), and LCK ( $P < 0.001$ ; Cor = 0.69) (Figure 7A) positively related to CD8<sup>+</sup> T cell and negatively correlated with tumor purity (Figure 7B). This

result suggested that M2 macrophages were negatively related to antigen processing.

## HPA

The prognostic value and immune phenotype correlation were determined for these M2 macrophage-related genes. We compared the various expression levels of these genes between normal and tumor tissues. HPA001804 is an antibody against F13A1, which showed higher intensity in tumor tissue than in normal tissue. HPA056371 is an antibody against FUCA1, which showed higher intensity in the normal tissue than in tumor tissue. CAB012245 is an antibody against SDCBP, which showed a higher intensity in tumor tissue than in normal tissue. HPA003903 is an antibody against VSIG4, which showed higher intensity in tumor tissue than in normal tissue. HPA031454 is an antibody against HLA-E, which showed lower intensity in tumor tissue than in normal tissue. HPA001312 is an antibody against TAP2, which showed lower intensity in tumor tissue than in normal tissue. The protein levels





of these M2 macrophage genes were similar to the results of prognosis analysis at the transcription level (Figure 8). Subsequently, the M2 correlations for VSIG4, FUCA1, F13A1, SDCBP, HLA-E, and TAP2 were verified in the four GEO datasets (Supplementary Figure 1).

## VSIG4

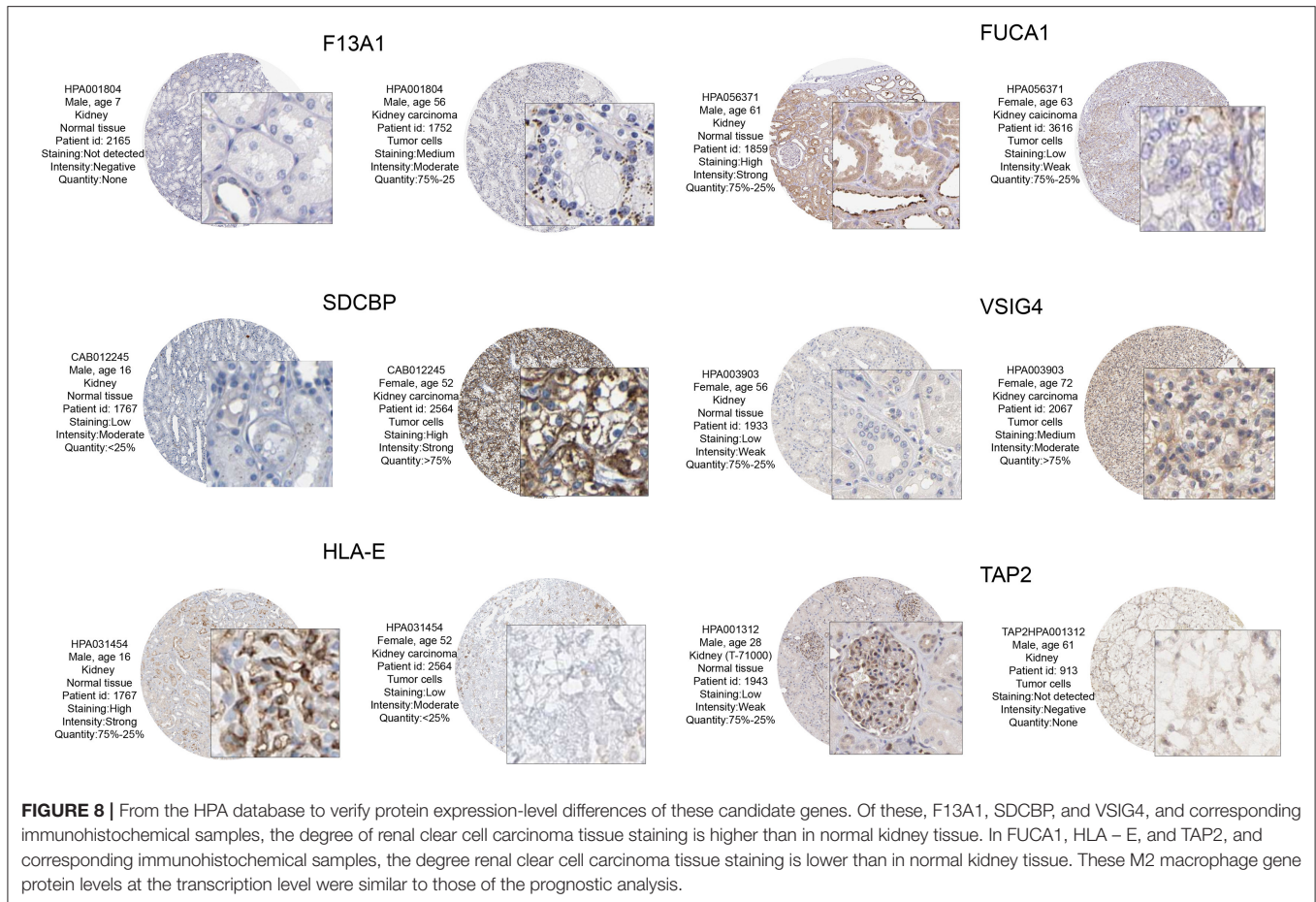
VSIG4 is thought to positively correlate with M2 macrophages; therefore, we conducted a combined analysis of VSIG4 and M2-type macrophages. Combining VSIG4 elevated the predictive accuracy of M2 macrophages even more than either of them alone; the hazard of the “high VSIG4 expression + high M2 macrophage” group showed more survival risk than the other group (Kaplan–Meier analysis, low VSIG4 expression + low M2 macrophage; HR = 1.458; Figure 9A). Subsequently, we compared VSIG4 protein expression levels between normal renal tissues and clear renal cell carcinoma and found that VSIG4 protein expression levels in tumors were higher than the normal tissues (Figure 9B). Then, various tumor infiltration

deconvolution methods were applied; we found that VSIG4 was one of the most commonly associated M2 macrophage biomarkers (Figure 9C).

## DISCUSSION

In the tumor microenvironment, the chemotactic effects of the functional differences between the types of tumor-associated macrophages are not completely clear. The biological cytological role of M2/M1 macrophages in tumor tissues still needs to be explored. The present study is based on a bioinformatics algorithm to determine some of the M2 macrophage co-expression networks. Through the analysis of various modules, we tried to explain the biological function of co-expressed genes with M2 macrophages and related pathway changes from the perspective of bioinformatics. Our data processing and analysis processes are shown in the flowchart (Figure 1).

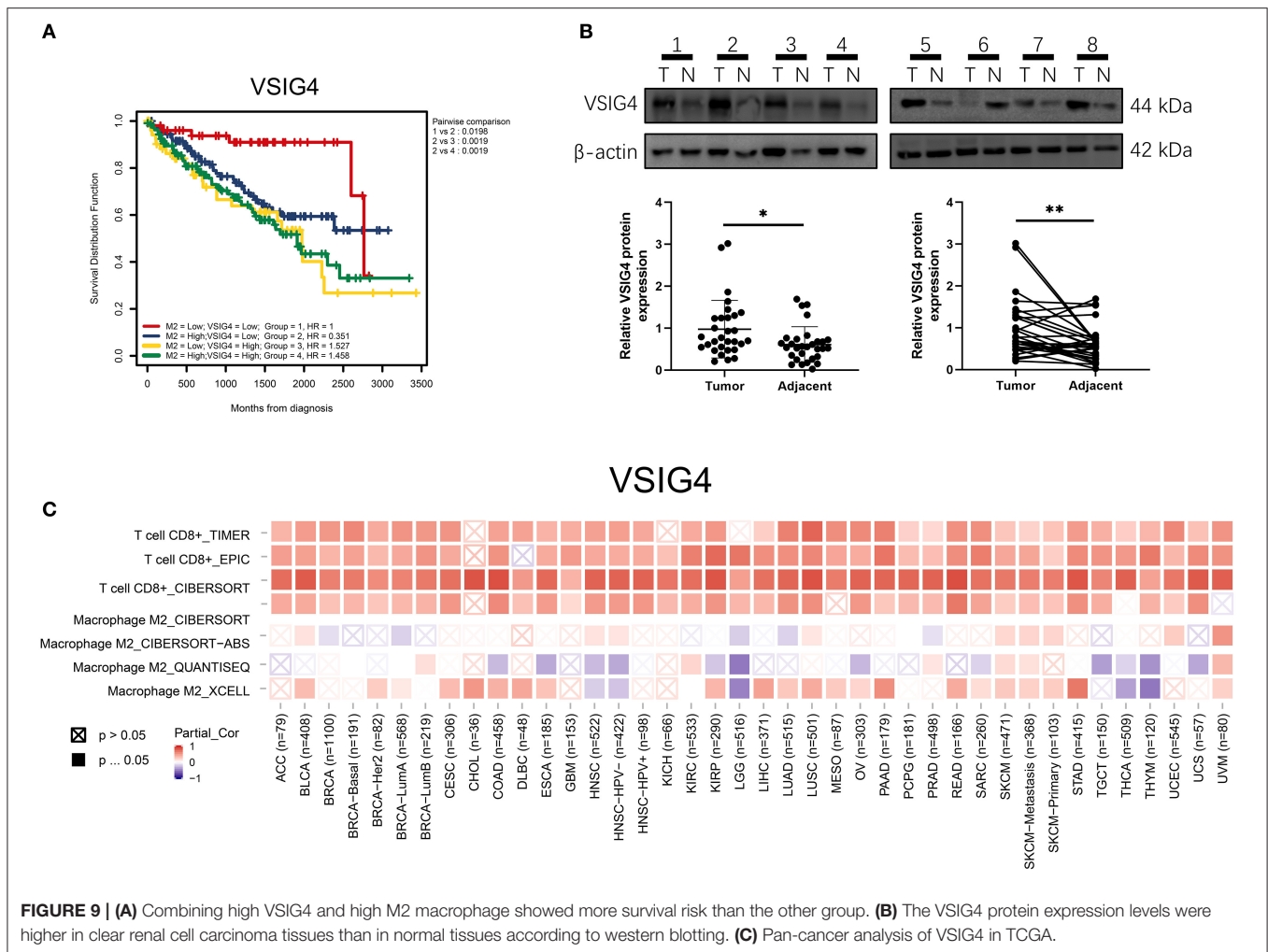
F13A1, FUCA1, HLA-E, VSIG4, SDCBP, and TAP2 were the most common co-expressed genes in M2 macrophages. In terms



of function enrichment, the 24 negatively co-expressed genes in M2 macrophages were most significantly enriched in antigen processing and presentation of exogenous peptide antigen via MHC class I. The 16 negatively co-expressing genes in M2 macrophages were most significantly enriched in neutrophil activation involved in immune response. M1 macrophages tend to adopt a Th1 response gene expression pattern and can secrete various cytokines that present MHC II and B7 molecules so as to present antigen efficiently (Herberman et al., 1979). This mechanism resists pathogen invasion, monitors tumor pathological changes, and generates Th1 immune responses in macrophages. By contrast, M2 macrophages have poor tumor antigen processing ability.

F13A1 encodes the coagulation factor XIII A subunit which has a catalytic function. In a human stem cell study, mRNA transcription expressed by F13A1 increased as myeloid progenitors differentiated into macrophages and erythroblasts (De Paoli et al., 2015). The protein encoded by FUCA1 is a lysosomal enzyme involved in the degradation of fucose-containing glycoproteins and glycolipids. Downregulation of FUCA1 enhances autophagy and inhibits macrophage infiltration so as to inhibit tumor growth (Xu L. et al., 2020). VSIG4 is a transmembrane receptor of the

immunoglobulin superfamily that is specifically expressed in macrophages and mature dendritic cells. It is a newly discovered B7 family-related macrophage protein that inhibits T cell activation and has a potential role in cancer (Kim et al., 2016). VSIG4 negatively regulates macrophage activation by reprogramming mitochondrial pyruvate metabolism (Li et al., 2017). HLA-E belongs to the HLA class I heavy chain paralogs. This class I molecule is a heterodimer consisting of a heavy chain and a light chain (beta-2 microglobulin). The heavy chain is anchored in the membrane. HLA-E binds a restricted subset of peptides derived from the leader peptides of other class I molecules. HLA-E is a non-classical HLA-I molecule that is best known for its role in protecting natural killer cells. Camilli et al. found that HLA-E was significantly increased during the differentiation of monocytes and macrophages (Camilli et al., 2016). The expression of HLA-E is related to the poor clinical results of anti-PD-1 immunotherapy. From the surface of M2 tumor-associated macrophages (TAMs), HLA-E antigen binds to the receptor CD94/NKG2A, which inhibits the expression of NK cell subpopulations and activated cytotoxic T lymphocytes, protecting cells from being destroyed (Marchesi et al., 2013). Epithelial-derived cancer cells, tumor macrophages, and CD141<sup>+</sup> traditional dendritic



cells promote the enrichment of HLA-E in carcinomas. CD8<sup>+</sup> tumor-infiltrating T lymphocytes with high PD-1 content are prevented from surviving in the tumor microenvironment by the interaction of enriched HLA-E and CD94/NKG2A inhibition (Abd Hamid et al., 2019).

This study has some limitations, including lack of cross-validation of multicenter data. There is also lack of experimental verification of M2 macrophage biomarkers in renal clear cell cancer. We found that using the co-expression method of network-building, we can explicitly identify biomarkers, demonstrating the correctness of the logic based on bioinformatics.

In conclusion, we found that F13A1, FCUA1, HLA-E, VSIG4, SDCBP, and TAP2 were biomarkers of M2-type macrophages using a co-expression network of infiltrated immune cells, and we proposed six candidate-related factors. The biomarkers and related processes of M2 macrophages in the tumor microenvironment were explained from the perspective of bioinformatics, providing a strategy to explore the polarization of macrophages.

## DATA AVAILABILITY STATEMENT

Publicly available datasets were analyzed in this study. This data can be found here: The TCGA-BLCA dataset used in this study were obtained from TCGA database (<https://cancergenome.nih.gov/>). GEO datasets used in this study were obtained from GEO database (<https://www.ncbi.nlm.nih.gov/geo/>).

## ETHICS STATEMENT

The studies involving human participants were reviewed and approved by The First Affiliated Hospital of China Medical University. The patients/participants provided their written informed consent to participate in this study.

## AUTHOR CONTRIBUTIONS

YW, KY, and JB designed the study. YW, KY, JLin, JLi, and JB analyzed and wrote the article.

All authors read and agreed to the final version of the manuscript.

## FUNDING

This work was supported by the China Shenyang Science and Technology Plan (20-205-4-015).

## ACKNOWLEDGMENTS

We appreciate the free use of TCGA and GEO databases.

## REFERENCES

- Abd Hamid, M., Wang, R. Z., Yao, X., Fan, P., Li, X., Chang, X. M., et al. (2019). Enriched HLA-E and CD94/NKG2A interaction limits antitumor CD8+ tumor-infiltrating T lymphocyte responses. *Cancer Immunol. Res.* 7, 1293–1306. doi: 10.1158/2326-6066.CIR-18-0885
- Ashburner, M., Ball, C. A., Blake, J. A., Botstein, D., Butler, H., Cherry, J. M., et al. (2000). Gene ontology: tool for the unification of biology. The Gene Ontology Consortium. *Nat. Genet.* 25, 25–29. doi: 10.1038/75556
- Camilli, G., Cassotta, A., Battella, S., Palmieri, G., Santoni, A., Paladini, F., et al. (2016). Regulation and trafficking of the HLA-E molecules during monocyte-macrophage differentiation. *J. Leukoc. Biol.* 99, 121–130. doi: 10.1189/jlb.1A0415-172R
- Cervantes-Villagrana, R. D., Albores-García, D., Cervantes-Villagrana, A. R., and García-Acevez, S. J. (2020). Tumor-induced neurogenesis and immune evasion as targets of innovative anti-cancer therapies. *Signal Transduct. Target Ther.* 5:99. doi: 10.1038/s41392-020-0205-z
- Chen, B., Khodadoust, M. S., Liu, C. L., Newman, A. M., and Alizadeh, A. A. (2018). Profiling tumor infiltrating immune cells with CIBERSORT. *Methods Mol. Biol.* 1711, 243–259. doi: 10.1007/978-1-4939-7493-1\_12
- Chowdhury, N., and Drake, C. G. (2020). Kidney cancer: an overview of current therapeutic approaches. *Urol. Clin. North Am.* 47, 419–431. doi: 10.1016/j.ucl.2020.07.009
- De Paoli, F., Eeckhoutte, J., Copin, C., Vanhoutte, J., Duhem, C., Derudas, B., et al. (2015). The neuron-derived orphan receptor 1 (NOR1) is induced upon human alternative macrophage polarization and stimulates the expression of markers of the M2 phenotype. *Atherosclerosis* 241, 18–26. doi: 10.1016/j.atherosclerosis.2015.04.798
- DeNardo, D. G., and Ruffell, B. (2019). Macrophages as regulators of tumour immunity and immunotherapy. *Nat. Rev. Immunol.* 19, 369–382. doi: 10.1038/s41577-019-0127-6
- Díaz-Montero, C. M., Rini, B. I., and Finke, J. H. (2020). The immunology of renal cell carcinoma. *Nat. Rev. Nephrol.* 16, 721–735. doi: 10.1038/s41581-020-0316-3
- Herberman, R. B., Holden, H. T., Djeu, J. Y., Jerrells, T. R., Varesio, L., Tagliabue, A., et al. (1979). Macrophages as regulators of immune responses against tumors. *Adv. Exp. Med. Biol.* 121B, 361–379. doi: 10.1007/978-1-4684-8914-9\_35
- Hsieh, J. J., Purdue, M. P., Signoretti, S., Swanton, C., Albiges, L., Schmidinger, M., et al. (2017). Renal cell carcinoma. *Nat. Rev. Dis. Primers* 3:17009. doi: 10.1038/nrdp.2017.9
- Huang, D. W., Sherman, B. T., Tan, Q., Collins, J. R., Alvord, W. G., Roayaei, J., et al. (2007). The DAVID Gene Functional Classification Tool: a novel biological module-centric algorithm to functionally analyze large gene lists. *Genome Biol.* 8:R183. doi: 10.1186/gb-2007-8-9-r183
- Jiang, J., Sun, X., Wu, W., Li, L., Wu, H., Zhang, L., et al. (2017). Corrigendum: Construction and application of a co-expression network in Mycobacterium tuberculosis. *Sci. Rep.* 7:40563. doi: 10.1038/srep40563
- Kanehisa, M., Furumichi, M., Tanabe, M., Sato, Y., and Morishima, K. (2017). KEGG: new perspectives on genomes, pathways, diseases and drugs. *Nucleic Acids Res.* 45, D353–D361. doi: 10.1093/nar/gkw1092

## SUPPLEMENTARY MATERIAL

The Supplementary Material for this article can be found online at: <https://www.frontiersin.org/articles/10.3389/fgene.2021.615655/full#supplementary-material>

**Supplementary Figure 1 | (A)** The multi-dataset correction of GSE8050, GSE12606, GSE14762, and GSE36895 using the “sva” package. **(B)** The verification analysis of M2 related genes in the combined cohorts.

**Supplementary Table 1 |** The detail information of tumor mutation, tumor purity, and M2 macrophage proportion.

**Supplementary Table 2 |** The process data of multi-Cox regression risk score model.

- Karnevi, E., Andersson, R., and Rosendahl, A. H. (2014). Tumour-educated macrophages display a mixed polarisation and enhance pancreatic cancer cell invasion. *Immunol. Cell Biol.* 92, 543–552. doi: 10.1038/icb.2014.22
- Kim, K. H., Choi, B. K., Kim, Y. H., Han, C., Oh, H. S., Lee, D. G., et al. (2016). Extracellular stimulation of VSIG4/complement receptor Ig suppresses intracellular bacterial infection by inducing autophagy. *Autophagy* 12, 1647–1659. doi: 10.1080/15548627.2016.1196314
- Langfelder, P., and Horvath, S. (2008). WGCNA: an R package for weighted correlation network analysis. *BMC Bioinformatics* 9:559. doi: 10.1186/1471-2105-9-559
- Lawrence, T., and Natoli, G. (2011). Transcriptional regulation of macrophage polarization: enabling diversity with identity. *Nat. Rev. Immunol.* 11, 750–761. doi: 10.1038/nri3088
- Leek, J. T., Johnson, W. E., Parker, H. S., Jaffe, A. E., and Storey, J. D. (2012). The sva package for removing batch effects and other unwanted variation in high-throughput experiments. *Bioinformatics* 28, 882–883. doi: 10.1093/bioinformatics/bts034
- Li, J., Diao, B., Guo, S., Huang, X., Yang, C., Feng, Z., et al. (2017). VSIG4 inhibits proinflammatory macrophage activation by reprogramming mitochondrial pyruvate metabolism. *Nat. Commun.* 8:1322. doi: 10.1038/s41467-017-01327-4
- Li, Y., Chen, Z., Wu, L., and Tao, W. (2020). Novel tumor mutation score versus tumor mutation burden in predicting survival after immunotherapy in pancreatic cancer patients from the MSK-IMPACT cohort. *Ann. Transl. Med.* 8:446. doi: 10.21037/atm.2020.03.163
- Linehan, W. M., and Ricketts, C. J. (2019). The Cancer Genome Atlas of renal cell carcinoma: findings and clinical implications. *Nat. Rev. Urol.* 16, 539–552. doi: 10.1038/s41585-019-0211-5
- Marchesi, M., Andersson, E., Villabona, L., Seliger, B., Lundqvist, A., Kiessling, R., et al. (2013). HLA-dependent tumour development: a role for tumour associated macrophages. *J. Transl. Med.* 11:247. doi: 10.1186/1479-5876-11-247
- Motzer, R. J., Hutson, T. E., Cella, D., Reeves, J., Hawkins, R., Guo, J., et al. (2013). Pazopanib versus sunitinib in metastatic renal-cell carcinoma. *N. Engl. J. Med.* 369, 722–731. doi: 10.1056/NEJMoa1303989
- Peña-Llopis, S., Vega-Rubín-de-Celis, S., Liao, A., Leng, N. A., Pavia-Jiménez, Wang, S., et al. (2012). BAP1 loss defines a new class of renal cell carcinoma. *Nat. Genet.* 44, 751–759. doi: 10.1038/ng.2323
- Pollard, J. W. (2004). Tumour-educated macrophages promote tumour progression and metastasis. *Nat. Rev. Cancer* 4, 71–78. doi: 10.1038/nrc1256
- Prapp, A. H. (2018). [Pearson's or Spearman's correlation coefficients]. *Tidsskr. Nor. Laegeforen.* 138:42. doi: 10.4045/tidsskr.18.0042
- Stickel, J. S., Weinzierl, A. O., Hillen, N., Drews, O., Schuler, M. M., Hennenlotter, J., et al. (2009). HLA ligand profiles of primary renal cell carcinoma maintained in metastases. *Cancer Immunol. Immunother.* 58, 1407–1417. doi: 10.1007/s00262-008-0655-6
- Uhlén, M., Fagerberg, L., Hallström, B. M., Lindskog, C., Oksvold, P., Mardinoglu, A., et al. (2015). Proteomics. Tissue-based map of the human proteome. *Science* 347:1260419. doi: 10.1126/science.1260419
- Wang, C., Wang, Y., Hong, T., Ye, J., Chu, C., Zuo, L., et al. (2020). Targeting a positive regulatory loop in the tumor-macrophage interaction impairs the progression of clear cell renal cell carcinoma. *Cell Death Differ.* doi: 10.1038/s41418-020-00626-6

- Wang, Y., Roche, O., Yan, M. S., Finak, G., Evans, A. J., Metcalf, J. L., et al. (2009). Regulation of endocytosis via the oxygen-sensing pathway. *Nat. Med.* 15, 319–324. doi: 10.1038/nm.1922
- Wang, Y., Yan, K., Lin, J., Wang, J., Zheng, Z., Li, X., et al. (2020). Three-gene risk model in papillary renal cell carcinoma: a robust likelihood-based survival analysis. *Aging* 12, 21854–21873. doi: 10.18632/aging.104001
- Weinzierl, A. O., Maurer, D., Altenberend, F., Schneiderhan-Marra, N., Klingel, K., Schoor, O., et al. (2008). A cryptic vascular endothelial growth factor T-cell epitope: identification and characterization by mass spectrometry and T-cell assays. *Cancer Res.* 68, 2447–2454. doi: 10.1158/0008-5472.CAN-07-2540
- Xu, L., Li, Z., Song, S., Chen, Q., Mo, L., Wang, C., et al. (2020). Downregulation of  $\alpha$ -L-fucosidase 1 suppresses glioma progression by enhancing autophagy and inhibiting macrophage infiltration. *Cancer Sci.* 111, 2284–2296. doi: 10.1111/cas.14427
- Xu, W., Atkins, M. B., and McDermott, D. F. (2020). Checkpoint inhibitor immunotherapy in kidney cancer. *Nat. Rev. Urol.* 17, 137–150. doi: 10.1038/s41585-020-0282-3
- Yang, Z., Wei, S., Deng, Y., Wang, Z., and Liu, L. (2020). Clinical significance of tumour mutation burden in immunotherapy across multiple cancer types: an individual meta-analysis. *Jpn. J. Clin. Oncol.* 50, 1023–1031. doi: 10.1093/jjco/hyaa076
- Yoshihara, K., Shahmoradgoli, M., Martinez, E., Vegesna, R., Kim, H., et al. (2013). Inferring tumour purity and stromal and immune cell admixture from expression data. *Nat. Commun.* 4:2612. doi: 10.1038/ncomms3612

**Conflict of Interest:** The authors declare that the research was conducted in the absence of any commercial or financial relationships that could be construed as a potential conflict of interest.

Copyright © 2021 Wang, Yan, Lin, Li and Bi. This is an open-access article distributed under the terms of the Creative Commons Attribution License (CC BY). The use, distribution or reproduction in other forums is permitted, provided the original author(s) and the copyright owner(s) are credited and that the original publication in this journal is cited, in accordance with accepted academic practice. No use, distribution or reproduction is permitted which does not comply with these terms.